

# PSEUDOSPIN $S = 1$ FORMALISM AND SKYRMION-LIKE EXCITATIONS IN THE THREE-BODY CONSTRAINED EXTENDED BOSE–HUBBARD MODEL

*A. S. Moskvina*\*

*Ural Federal University  
620083, Ekaterinburg, Russia*

Received March 30, 2015

We discuss the most prominent and intensively studied  $S = 1$  pseudospin formalism for the extended boson Hubbard model (EBHM) with the on-site Hilbert space truncated to the three lowest occupation states  $n = 0, 1, 2$ . The EBHM Hamiltonian is a paradigmatic model for the highly topical field of ultracold gases in optical lattices. The generalized non-Heisenberg effective pseudospin Hamiltonian does provide a deep link with a boson system and a physically clear description of “the myriad of phases”, from uniform Mott insulating phases and density waves to two types of superfluids and supersolids. We argue that the 2D pseudospin system is prone to a topological phase separation and focus on several types of unconventional skyrmion-like topological structures in 2D boson systems, which have not been analyzed until now. The structures are characterized by a complicated interplay of insulating and two superfluid phases with a single-boson and two-boson condensation, respectively.

DOI: 10.7868/S0044451015090126

## 1. INTRODUCTION

Since 1989, the bosonic Hubbard model (see [1] and the references therein) has attracted continued interest due to its very rich ground-state phase diagram and great opportunities of direct experimental realization in systems of ultracold boson atoms loaded in optical lattices. Such systems offer unique opportunities for studying strongly correlated quantum matter in a highly controllable environment.

The Hamiltonian of the extended boson Hubbard model (EBHM) is usually defined as

$$H = - \sum_{i>j} t_{ij} (\hat{b}_i^\dagger \hat{b}_j + \text{H.c.}) + \frac{U}{2} \sum_i \hat{n}_i (\hat{n}_i - 1) + \sum_{i>j} V_{ij} \hat{n}_i \hat{n}_j - \mu \sum_i \hat{n}_i, \quad (1)$$

where  $\hat{b}_i^\dagger$ ,  $\hat{b}_i$ , and  $\hat{n}_i = \hat{b}_i^\dagger \hat{b}_i$  are respectively the boson creation, annihilation, and number operators at the lattice site  $i$ . The boson transfer amplitudes are given by  $t_{ij}$ ;  $U_i = U$  and  $V_{ij}$  parameterize the Coulomb repulsions between bosons located at the same and different

sites. While  $t_{ij}$  causes the bosons to delocalize, promoting a superfluid (SF) phase at weak interactions,  $U$  and  $V_{ij}$  tend to stabilize the conventional Mott insulator (MI) and the density wave (DW) phases when the interaction dominates over the hopping energy scale set by  $t$ .

Attractive on-site boson–boson interactions allow for the formation of dimers, or bound states of two bosons. The phase diagram then contains the conventional one-boson superfluid (1-BS) with nonvanishing order parameters  $\langle \hat{b}_j \rangle \neq 0$  and  $\langle \hat{b}_j^2 \rangle \neq 0$  and the dimer superfluid (2-BS) phase. The 2-BS phase is characterized by the vanishing of the one-boson order parameter ( $\langle \hat{b}_j \rangle = 0$ ) but has a nonzero pairing correlation ( $\langle \hat{b}_j^2 \rangle \neq 0$ ). Apart from the above local order parameters, one can use superfluid stiffness to identify the superfluid states. We note that thermal transitions between the 2-BS dimer superfluid and the 1-BS normal fluid are considered in Ref. [2].

When the inter-site boson–boson repulsion is turned on, in addition to the uniform Mott insulating (MI) state and two superfluid phases, a dimer checkerboard solid state appears at unit filling, where boson pairs form a solid with a checkerboard structure.

\*E-mail: alexander.moskvina@urfu.ru

Our starting point for theoretical analysis of the 2D extended Bose–Hubbard model is to assume truncation of the on-site Hilbert space to the three lowest-occupation states  $n = 0, 1, 2$  with a further mapping of the EBHM Hamiltonian to an anisotropic spin-1 model (see, e. g., [3]). The simplest effective spin-1 model Hamiltonian is

$$\hat{H} = - \sum_{i>j} t_{ij} (S_{ix} S_{jx} + S_{iy} S_{jy}) + \frac{U}{2} \sum_i S_{iz}^2 + \sum_{i>j} V_{ij} S_{iz} S_{jz} - \mu \sum_i S_{iz}. \quad (2)$$

In this space, the DW phase corresponds to an antiferromagnetic ordering of the pseudospins in the  $z$  direction. The MI ground state, on the other hand, includes a large amplitude of the state with  $M_S = 0$  on every site with a small admixture of states containing tightly bound particle–hole fluctuations ( $M_S = \pm 1$  on nearby sites). The phase can be termed a quantum paramagnet. The 1-BS and 2-BS superfluid phases respectively correspond to the dipole and quadrupole (nematic) pseudospin XY-order. Generally speaking, we may anticipate the emergence of so-called supersolid phases, or mixed 1-BS+DW (2-BS+DW) phases.

In this paper, we consider the most general form of the effective  $S = 1$  pseudospin Hamiltonian related to the extended Bose–Hubbard model and present a short overview of different phase states. We focus on several types of unconventional skyrmion-like topological structures in 2D boson systems, which have not been analyzed until now. The structures are characterized by a complicated interplay of insulating and two superfluid phases. The rest of the paper is organized as follows. Section 2 is an introduction into the pseudospin formalism. In Sec. 3, we introduce and analyze the effective pseudospin Hamiltonian. In Sec. 4, we turn to a short overview of a typical simplified  $S = 1$  spin model. Unconventional pseudospin topological structures are considered in Sec. 5, with a short conclusion in Sec. 6.

## 2. PSEUDOSPIN FORMALISM

One strategy to deal with the physics of the extended Bose–Hubbard model with the on-site Hilbert space truncated to  $n = 0, 1, 2$  is to use an  $S = 1$  pseudospin formalism [4, 5] and to create a model pseudospin Hamiltonian that can reproduce both the ground state and important low-energy excitations of the full problem reasonably well. The standard pseudospin formalism represents a variant of the equivalent-

operator technique widely known in different physical problems, from classical and quantum lattice gases, binary alloys, (anti)ferroelectrics, etc., to neural networks. The formalism starts with a finite basis set for a lattice site (triplet in our model). Such an approach differs from well-known pseudospin–particle transformations akin to Jordan–Wigner [6] or Holstein–Primakoff [7] transformations that establish a strict link between pseudospin operators and the creation/annihilation operators of the Fermi or Bose type. The pseudospin formalism generally proceeds with a truncated basis and does not imply a strict relation to boson operators that obey the boson commutation rules.

The three on-site Fock states  $|n = 0\rangle$ ,  $|n = 1\rangle$ , and  $|n = 2\rangle$  form a local Hilbert space of the semi-hard core bosons, which can be mapped onto a system of  $S = 1$  centers via a generalization of the Matsubara–Matsuda transformation [5] that also maps the boson density into the local magnetization:  $n_j = S_{zj} + 1$ . In contrast to the hard-core bosons associated with  $S = 1/2$  magnets, it is possible to study “Hubbard-like” boson gases with on-site density–density (contact) interactions because  $n_j \leq 2$ . Hereafter, we relate the three on-site Fock states with the occupation numbers  $n = 0, 1, 2$  to the three components of the  $S = 1$  pseudospin (isospin) triplet with  $M_S = -1, 0, +1$ , respectively. It is worth noting that a very similar  $S = 1$  pseudospin formalism was suggested recently [8, 9] to describe the triplet of  $\text{Cu}^{1+}$ ,  $\text{Cu}^{2+}$ ,  $\text{Cu}^{3+}$  valence states in high-temperature copper superconductors.

The  $S = 1$  spin algebra includes the three independent irreducible tensors  $\hat{V}_q^k$  of rank  $k = 0, 1, 2$  with one, three, and five components respectively, obeying the Wigner–Eckart theorem [10]

$$\langle SM | \hat{V}_q^k | SM' \rangle = (-1)^{S-M} \begin{pmatrix} S & k & S \\ -M & q & M' \end{pmatrix} \langle S || \hat{V}^k || S \rangle. \quad (3)$$

Here, we use standard symbols for the Wigner coefficients and reduced matrix elements. In a more conventional Cartesian scheme, a complete set of nontrivial pseudospin operators would include both  $\mathbf{S}$  and a number of symmetrized bilinear forms  $\{S_i S_j\} = (S_i S_j + S_j S_i)$ , or spin-quadrupole operators, which are linearly related to  $V_q^1$  and  $V_q^2$ :

$$V_q^1 = S_q; \quad S_0 = S_z, \quad S_{\pm} = \mp \frac{1}{\sqrt{2}} (S_x \pm i S_y); \\ V_0^2 \propto (3S_z^2 - \mathbf{S}^2), \quad V_{\pm 1}^2 \propto (S_z S_{\pm} + S_{\pm} S_z), \\ V_{\pm 2}^2 \propto S_{\pm}^2. \quad (4)$$

Instead of the three  $|1M\rangle$  states, one can use the Cartesian basis set  $\Psi$ , or  $|x, y, z\rangle$ :

$$|10\rangle = |z\rangle, \quad |1\pm 1\rangle = \mp \frac{1}{\sqrt{2}}(|x\rangle \pm i|y\rangle) \quad (5)$$

such that the on-site wave function can be written in the matrix form [11]

$$\psi = \begin{pmatrix} c_1 \\ c_2 \\ c_3 \end{pmatrix} = \begin{pmatrix} R_1 \exp(i\Phi_1) \\ R_2 \exp(i\Phi_2) \\ R_3 \exp(i\Phi_3) \end{pmatrix}, \quad |\mathbf{R}|^2 = 1, \quad (6)$$

with  $\mathbf{R} = \{\sin \Theta \cos \eta, \sin \Theta \sin \eta, \cos \Theta\}$ . Obviously, the minimal number of dynamic variables describing an isolated on-site  $S = 1$  (pseudo)spin center equals to four; however, for a more general situation, when the (pseudo)spin system represents only a part of the bigger system and we are forced to consider the coupling to the additional degrees of freedom, we should consider all the five nontrivial parameters.

The pseudospin matrix has a very simple form in terms of the  $|x, y, z\rangle$  basis set:

$$\langle i|\hat{S}_k|j\rangle = i\epsilon_{ikj}. \quad (7)$$

We start by introducing a set of  $S = 1$  coherent states characterized by vectors  $\mathbf{a}$  and  $\mathbf{b}$  satisfying the normalization constraint [11]

$$|\mathbf{c}\rangle = |\mathbf{a}, \mathbf{b}\rangle = \mathbf{c} \cdot \Psi = (\mathbf{a} + i\mathbf{b}) \cdot \Psi, \quad (8)$$

where  $\mathbf{a}$  and  $\mathbf{b}$  are real vectors that are arbitrarily oriented with respect to some fixed coordinate system in the pseudospin space with the orthonormal basis  $\mathbf{e}_{1,2,3}$ .

The two vectors are coupled, and therefore the minimal number of dynamic variables describing the  $S = 1$  (pseudo)spin system appears to be equal to four. We emphasize the *director* nature of the  $\mathbf{c}$  vector field:  $|\mathbf{c}\rangle$  and  $|-\mathbf{c}\rangle$  describe physically identical states.

We note that in real space, the  $|\mathbf{c}\rangle$  state corresponds to a quantum on-site superposition:

$$|\mathbf{c}\rangle = c_{-1}|0\rangle + c_0|1\rangle + c_{+1}|2\rangle. \quad (9)$$

The existence of such unconventional on-site superpositions is a principal point of the model. Below, instead of  $\mathbf{a}$  and  $\mathbf{b}$ , we use a pair of unit vectors  $\mathbf{m}$  and  $\mathbf{n}$  defined as follows [12]:

$$\mathbf{a} = \cos \varphi \mathbf{m}, \quad \mathbf{b} = \sin \varphi \mathbf{n}.$$

For the averages of the principal pseudospin operators, we obtain

$$\langle \mathbf{S} \rangle = \sin 2\varphi [\mathbf{m} \times \mathbf{n}],$$

$$\langle \{S_i, S_j\} \rangle = 2(\delta_{ij} - \cos^2 \varphi m_i m_j - \sin^2 \varphi n_i n_j), \quad (10)$$

or

$$\langle S_i^2 \rangle = 1 - \frac{1}{2}(m_i^2 + n_i^2) - \frac{1}{2}(m_i^2 - n_i^2) \cos 2\varphi,$$

$$\langle \{S_i, S_j\} \rangle = -(m_i m_j + n_i n_j) - (m_i m_j - n_i n_j) \cos 2\varphi \quad (i \neq j). \quad (11)$$

We note a principal difference between the  $S = 1/2$  and  $S = 1$  quantum systems. The only on-site order parameter in the former case is the average spin moment  $\langle S_{x,y,z} \rangle$ , whereas in the latter, we have five additional ‘‘spin-quadrupole’’, or spin-nematic order parameters described by the traceless symmetric tensors

$$Q_{ij} = \left\langle \left( \frac{1}{2} \{S_i, S_j\} - \frac{2}{3} \delta_{ij} \right) \right\rangle. \quad (12)$$

Interestingly, the  $S = 1/2$  quantum spin system, with all the order parameters defined by a simple on-site vectorial order parameter  $\langle \mathbf{S} \rangle$ , is in a sense closer to a classical one ( $S \rightarrow \infty$ ) than the  $S = 1$  quantum spin system, with its eight independent on-site order parameters.

The operators  $V_q^k$  ( $q \neq 0$ ) change the  $z$ -projection of the pseudospin and transform the  $|SM_S\rangle$  state into the  $|SM_S + q\rangle$  one. In other words, these operators can change the occupation number. We emphasize that in the  $S = 1$  pseudospin algebra, there are two operators,  $V_{\pm 1}^1$  and  $V_{\pm 1}^2$ , or  $S_{\pm}$  and  $T_{\pm} = \{S_z, S_{\pm}\}$ , that change the pseudospin projection (and the occupation number) by  $\pm 1$ , with slightly different properties:

$$\langle 0|\hat{S}_{\pm}|\mp 1\rangle = \langle \pm 1|\hat{S}_{\pm}|0\rangle = \mp 1, \quad (13)$$

but

$$\langle 0|\hat{T}_{\pm}|\mp 1\rangle = -\langle \pm 1|\hat{T}_{\pm}|0\rangle = +1. \quad (14)$$

It is worth noting similar behavior of both operators under Hermitian conjugation:  $\hat{S}_{\pm}^{\dagger} = -\hat{S}_{\mp}$ ;  $\hat{T}_{\pm}^{\dagger} = -\hat{T}_{\mp}$ .

The  $V_{\pm 2}^2$ , or  $\hat{S}_{\pm}^2$  operator changes the pseudospin projection by  $\pm 2$  with the local order parameter

$$\begin{aligned} \langle S_{\pm}^2 \rangle &= \frac{1}{2}(\langle S_x^2 - S_y^2 \rangle \pm i\langle \{S_x, S_y\} \rangle) = \\ &= c_+^* c_- = c_x^2 - c_y^2 \pm 2i c_x c_y. \end{aligned} \quad (15)$$

Obviously, this on-site off-diagonal order parameter is nonzero only when both  $c_+$  and  $c_-$  are nonzero, or for the on-site  $0-2$  superpositions. It is worth noting that the  $\hat{S}_+^2$  ( $\hat{S}_-^2$ ) operator creates an on-site boson pair, or a

dimer, with the kinematic constraint  $(\hat{S}_\pm^2)^2 = 0$ , which underlines its “hard-core” nature.

Figure 1 shows orientations of the  $\mathbf{m}$  and  $\mathbf{n}$  vectors that provide extremal values of different on-site pseudospin order parameters at  $\varphi = \pi/4$ . The  $n = 1$  center is described by a pair of  $\mathbf{m}$  and  $\mathbf{n}$  vectors directed along the  $Z$  axis with  $|m_z| = |n_z| = 1$ . We arrive at the respective  $1 - 2$  or  $1 - 0$  mixtures if we turn  $c_{-1}$  or  $c_{+1}$  into zero. The mixtures are described by a pair of  $\mathbf{m}$  and  $\mathbf{n}$  vectors whose projections on the  $XY$  plane,  $\mathbf{m}_\perp$  and  $\mathbf{n}_\perp$ , are of the same length and orthogonal to each other:  $\mathbf{m}_\perp \cdot \mathbf{n}_\perp = 0$ ,  $m_\perp = n_\perp$  with  $[\mathbf{m}_\perp \times \mathbf{n}_\perp] = \langle S_z \rangle = \pm \sin^2 \theta$  for  $1 - 2$  and  $1 - 0$  mixtures, respectively (see Fig. 1).

It is worth noting that for the “conical” configurations in Figs. 1b–1d, we have

$$\begin{aligned} \langle S_z \rangle &= 0; \quad \langle S_z^2 \rangle = \sin^2 \theta, \\ \langle S_\pm^2 \rangle &= -\frac{1}{2} \sin^2 \theta e^{\pm 2i\varphi}, \\ \langle S_\pm \rangle &= -\frac{i}{\sqrt{2}} \sin 2\theta e^{\pm i\varphi}, \quad \langle T_\pm \rangle = 0 \end{aligned} \quad (16)$$

(Fig. 1b);

$$\begin{aligned} \langle S_z \rangle &= 0, \quad \langle S_z^2 \rangle = \sin^2 \theta, \\ \langle S_\pm^2 \rangle &= -\frac{1}{2} \sin^2 \theta e^{\pm 2i\varphi}, \\ \langle S_\pm \rangle &= 0, \quad \langle T_\pm \rangle = \mp \frac{1}{\sqrt{2}} \sin 2\theta e^{\pm i\varphi} \end{aligned} \quad (17)$$

(Fig. 1c); and

$$\begin{aligned} \langle S_z \rangle &= -\langle S_z^2 \rangle = -\sin^2 \theta, \quad \langle S_\pm^2 \rangle = 0, \\ \langle S_\pm \rangle &= \langle T_\pm \rangle = \pm \frac{1}{2} e^{\mp i\frac{\pi}{4}} \sin 2\theta e^{\pm i\varphi} \end{aligned} \quad (18)$$

(Fig. 1d). Figures 1e,f show the orientation of the  $\mathbf{m}$  and  $\mathbf{n}$  vectors for the local binary mixture  $0 - 2$ , and Fig. 1g does so for  $n = 2$  center. It is worth noting that for binary mixtures  $|1\rangle - |0\rangle$  and  $|1\rangle - |2\rangle$ , we arrive at the same algebra of the  $\hat{S}_\pm$  and  $\hat{T}_\pm$  operators with  $\langle S_\pm \rangle = \langle T_\pm \rangle$ , while for ternary mixtures  $|0\rangle - |1\rangle - |2\rangle$ , these operators describe different excitations. Interestingly, in all cases, the local  $n = 1$  fraction can be written as

$$\rho(n = 1) = 1 - \langle S_z^2 \rangle = \cos^2 \theta. \quad (19)$$

In the boson language,  $\langle S_z \rangle$  and  $\langle S_z^2 \rangle$  are on-site diagonal order parameters that respectively describe the local density and boson nematic order. The on-site mean values  $\langle S_\pm \rangle$  and  $\langle T_\pm \rangle$  are the two types of local off-diagonal order parameters that describe one-boson superfluidity, while  $\langle S_\pm^2 \rangle$  is a local order parameter of the two-boson, or dimer superfluidity.

### 3. EFFECTIVE $S = 1$ PSEUDOSPIN HAMILTONIAN

The general form of the effective pseudospin Hamiltonian that commutes with the  $z$ -component of the total pseudospin  $\sum_i S_{iz}$  and hence preserves the mean boson density is [8, 9]

$$\begin{aligned} \hat{H} &= \sum_i (\Delta_i S_{iz}^2 - (\mu - h_i) S_{iz}) + \\ &+ \sum_{k_1 k_2 q} \sum_{i < j} I_{k_1 k_2 q}(ij) \hat{V}_q^{k_1}(i) \hat{V}_{-q}^{k_2}(j). \end{aligned} \quad (20)$$

The Hamiltonian can be rewritten as a sum of potential and kinetic energies, that is, of the  $q = 0$  (“diagonal”)  $\hat{H}_{ch}$  and  $q \neq 0$  (“off-diagonal”)  $\hat{H}_{tr}$  terms:

$$\hat{H} = \hat{H}_{ch} + \hat{H}_{tr}, \quad (21)$$

where

$$\begin{aligned} \hat{H}_{ch} &= \sum_i (\Delta_i S_{iz}^2 - (\mu - h_i) S_{iz}) + \\ &+ \sum_{i < j} V_{ij} (S_{iz} S_{jz} + \alpha S_{iz}^2 S_{jz}^2), \end{aligned} \quad (22)$$

and  $\hat{H}_{tr} = \hat{H}_{tr}^{(1)} + \hat{H}_{tr}^{(2)}$  are the sums of one-particle and two-particle transfer contributions

$$\begin{aligned} \hat{H}_{tr}^{(1)} &= \sum_{i < j} t_{ij}^S (S_{i+} S_{j-} + S_{i-} S_{j+}) + \\ &+ \sum_{i < j} t_{ij}^T (T_{i+} T_{j-} + T_{i-} T_{j+}) + \\ &+ \sum_{i < j} t_{ij}^{ST} (S_{i+} T_{j-} + S_{i-} T_{j+} + T_{i+} S_{j-} + T_{i-} S_{j+}); \end{aligned} \quad (23)$$

$$\hat{H}_{tr}^{(2)} = \sum_{i < j} t_{ij}^d (S_{i+}^2 S_{j-}^2 + S_{i-}^2 S_{j+}^2), \quad (24)$$

with the boson density constraint

$$\frac{1}{2N} \sum_i \langle S_{iz} \rangle = \Delta n, \quad (25)$$

where  $\Delta n$  is the deviation from half-filling ( $n = 1$ ).

The Hamiltonian  $\hat{H}_{ch}$  corresponds to a classical spin-1 Ising model with a single-ion anisotropy term, or the generalized Blume–Capel model [13], in the presence of a longitudinal magnetic field. The first single-site term in  $\hat{H}_{ch}$  describes the effects of a bare pseudospin splitting and relates to the on-site density–density interactions:  $\Delta = U$ . The second term can be related to a pseudomagnetic field  $\mathbf{h}_i \parallel Z$  that acts as

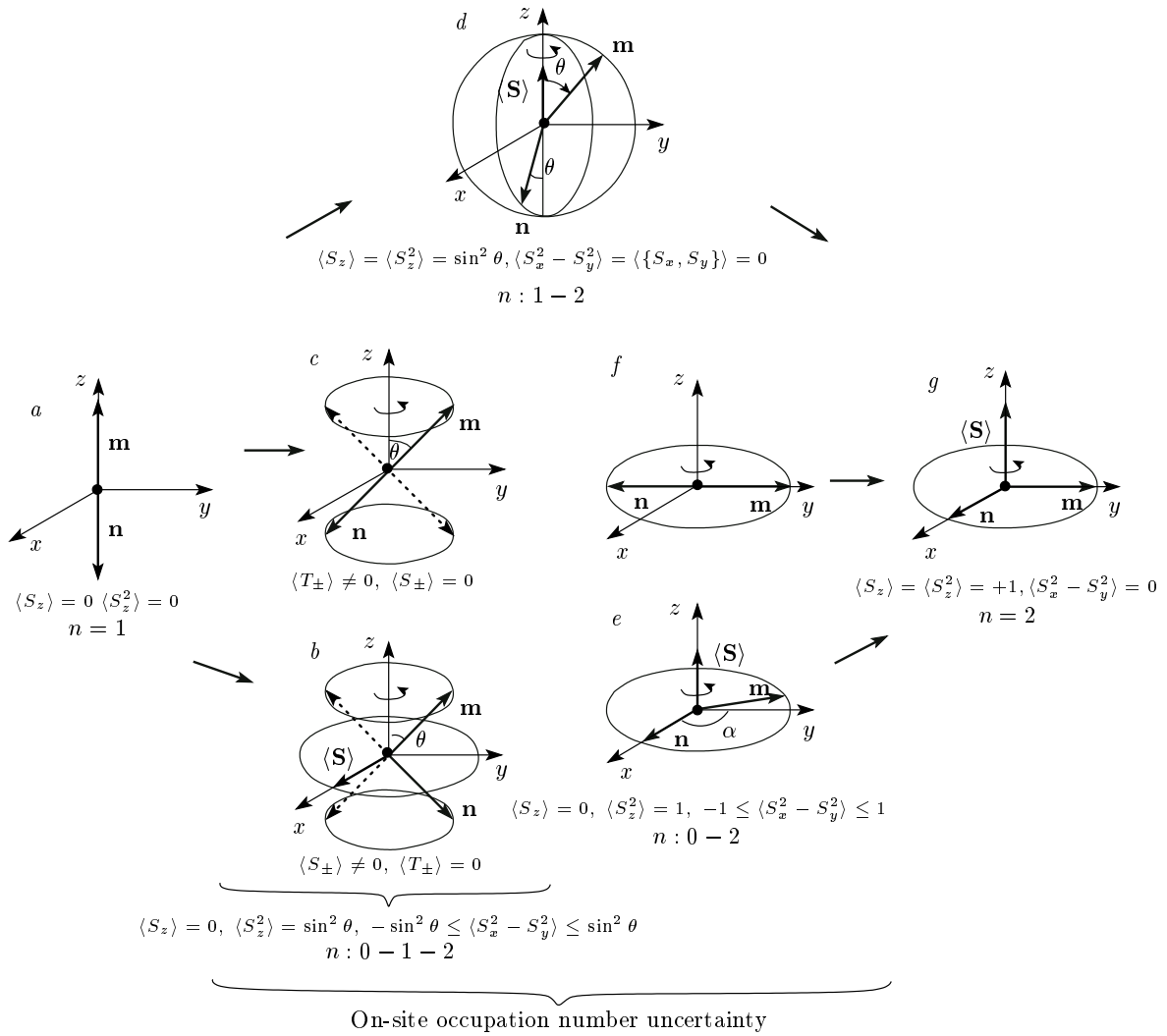


Fig. 1. Schematic showing orientations of the  $\mathbf{m}$  and  $\mathbf{n}$  vectors that provide extremal values of different on-site pseudospin order parameters for  $\varphi = \pi/4$

a chemical potential ( $\mu$  is the boson chemical potential and  $h_i$  is a (random) site energy). At variance with the real external field, the chemical potential depends on both the parameters of Hamiltonian (21) and the temperature. The third bilinear and fourth biquadratic terms in  $\hat{H}_{ch}$  describe the effects of the short- and long-range inter-site density-density interactions.

The Hamiltonian  $\hat{H}_{tr}$  plays the role of kinetic energy, with  $\hat{H}_{tr}^{(1)}$  and  $\hat{H}_{tr}^{(2)}$  respectively describing the one- and two-particle inter-site hopping. The Hamiltonian  $\hat{H}_{tr}^{(1)}$  represents an obvious extension of the conventional Hubbard model that assumes that the single-particle orbital is infinitely rigid irrespective of the occupation number, and has much in common with so-called dynamic Hubbard models [14] that describe a

correlated hopping. The ST and TT terms describe a density-dependent single-particle hopping. It was Hirsch and coworkers [14] who stressed the importance of density-induced tunneling effects in the condensed-matter context.

However, before mapping the pseudospin model into a discrete free boson model, we must verify that the amplitude of the one-particle hoppings in Bose-Hubbard Hamiltonian (1) obey the boson commutation relations. This implies that the amplitude of the  $|1\rangle|2\rangle \rightarrow |2\rangle|1\rangle$  process is twice as large as that of  $|0\rangle|1\rangle \rightarrow |1\rangle|0\rangle$  and a factor  $\sqrt{2}$  larger than that of  $|1\rangle|1\rangle \rightarrow |2\rangle|0\rangle$ . We note that in the triplet basis  $|0, 1, 2\rangle$ , the boson annihilation operator reads as [3]

$$\begin{aligned} \hat{b}_i &= \frac{1}{2} \left[ (1 + \sqrt{2}) \hat{S}_{i-} - (1 - \sqrt{2}) \hat{T}_{i-} \right] = \\ &= \sqrt{2} \left( 1 + \frac{\sqrt{2} - 1}{\sqrt{2}} \hat{S}_{iz} \right) \hat{S}_{i+}. \end{aligned} \quad (26)$$

In other words, in the framework of the standard EBHM approach, all the SS, TT, and ST terms in the pseudospin kinetic energy are governed by a single Hubbard transfer integral  $t$ :

$$\begin{aligned} t^S &= -\frac{(1 + \sqrt{2})^2}{4} t, & t^T &= -\frac{(1 - \sqrt{2})^2}{4} t, \\ t^{ST} &= -\sqrt{2} t, & t^d &= 0, \end{aligned} \quad (27)$$

while the pseudospin Hamiltonian  $\hat{H}_{tr}$  allows describing more complicated transfer mechanisms. The one- and two-particle hopping terms in  $\hat{H}_{tr}$  are of primary importance for the transport properties of our model system, and deserve special attention. Three (SS-, TT-, and ST-) types of the one-particle hopping terms are respectively governed by the three transfer integrals  $t_{ij}^S$ ,  $t_{ij}^T$ , and  $t_{ij}^{ST}$ . Instead of  $\hat{S}_{\pm}$  and  $\hat{T}_{\pm}$ , we can introduce two novel operators  $\hat{P}_{\pm}$  and  $\hat{N}_{\pm}$  as

$$\hat{P}_{\pm} = \frac{1}{2}(\hat{S}_{\pm} + \hat{T}_{\pm}), \quad \hat{N}_{\pm} = \frac{1}{2}(\hat{S}_{\pm} - \hat{T}_{\pm}). \quad (28)$$

Then the single-particle transfer Hamiltonian becomes

$$\begin{aligned} \hat{H}_{tr}^{(1)} &= \sum_{i<j} t_{ij}^P (P_{i+} P_{j-} + P_{i-} P_{j+}) + \\ &+ \sum_{i<j} t_{ij}^N (N_{i+} N_{j-} + N_{i-} N_{j+}) + \sum_{i<j} t_{ij}^{PN} (P_{i+} N_{j-} + \\ &+ P_{i-} N_{j+} + N_{i+} P_{j-} + N_{i-} P_{j+}), \end{aligned} \quad (29)$$

where

$$\begin{aligned} t_{ij}^P &= t_{ij}^S + t_{ij}^T + t_{ij}^{ST}, & t_{ij}^N &= t_{ij}^S + t_{ij}^T - t_{ij}^{ST}, \\ t_{ij}^{PN} &= t_{ij}^S - t_{ij}^T. \end{aligned} \quad (30)$$

All the three terms here have a clear physical interpretation. The first,  $PP$ -type term describes one-particle hopping processes  $|1\rangle |2\rangle \rightarrow |2\rangle |1\rangle$ , which are a rather conventional motion of the extra boson in the lattice with the  $n = 1$  on-site occupation or the motion of a boson hole in the lattice with the  $n = 2$  on-site occupation. The second,  $NN$ -type term describes one-particle hopping processes  $|1\rangle |0\rangle \rightarrow |0\rangle |1\rangle$ , which are a rather conventional motion of a boson hole in the lattice with the  $n = 1$  on-site occupation or the motion of a boson in the lattice with the  $n = 0$  on-site occupation. These hopping processes are respectively typical for heavily underfilled ( $\langle n \rangle \ll 1$ ) or heavily overfilled ( $\langle n \rangle \leq 2$ )

lattices. It is worth noting that the ST-type contribution of the one-particle transfer differs in sign for the  $PP$  and  $NN$  transfer, thus breaking the ‘‘particle–hole’’ symmetry.

The third,  $PN$  ( $NP$ ), term in (29) defines a very different one-particle hopping process,  $|1\rangle |1\rangle \rightarrow |2\rangle |0\rangle$  ( $|0\rangle |2\rangle$ ), which is the particle–hole creation/annihilation. We note that the ST-type transfer does not contribute to the reaction.

The two-particle(hole), or dimer hopping is governed by the transfer integral  $t_{ij}^d$  that defines the probability amplitude for the ‘‘exchange’’ reaction  $|0\rangle |2\rangle \rightarrow |2\rangle |0\rangle$ , either the motion of an on-site dimer in the lattice with the  $n = 0$  on-site occupation or the motion of an on-site hole  $n = 0$  in the lattice with the  $n = 2$  on-site occupation.

All the kinetic energies can be rewritten in terms of the Cartesian pseudospin components if we take into account that

$$\begin{aligned} (S_{i+} S_{j-} + S_{i-} S_{j+}) &= -(S_{ix} S_{jx} + S_{iy} S_{jy}), \\ (S_{i+} S_{j-} - S_{i-} S_{j+}) &= i(S_{ix} S_{jy} - S_{iy} S_{jx}) = i[\mathbf{S}_1 \times \mathbf{S}_2]_z, \end{aligned}$$

$$\begin{aligned} (T_{i+} T_{j-} + T_{i-} T_{j+}) &= -(T_{ix} T_{jx} + T_{iy} T_{jy}) = \\ &= -(S_{ix} S_{jx} + S_{iy} S_{jy}) S_{iz} S_{jz} - \\ &- S_{iz} (S_{ix} S_{jx} + S_{iy} S_{jy}) S_{jz} + \text{H.c.}, \end{aligned}$$

$$(T_{i+} T_{j-} - T_{i-} T_{j+}) = i(T_{ix} T_{jy} - T_{iy} T_{jx}) = i[\mathbf{T}_1 \times \mathbf{T}_2]_z,$$

$$\begin{aligned} (S_{i+} T_{j-} + S_{i-} T_{j+}) + \text{H.c.} &= \\ &= -\{(S_{iz} + S_{jz}), (S_{ix} S_{jx} + S_{iy} S_{jy})\}, \end{aligned}$$

$$\begin{aligned} (S_{i+}^2 S_{j-}^2 + S_{i-}^2 S_{j+}^2) &= \\ = \frac{1}{2} [(S_{ix}^2 - S_{iy}^2)(S_{jx}^2 - S_{jy}^2) + \{S_{ix}, S_{iy}\} \{S_{jx}, S_{jy}\}], \end{aligned}$$

$$\begin{aligned} (S_{i+}^2 S_{j-}^2 - S_{i-}^2 S_{j+}^2) &= -\frac{i}{2} [(S_{ix}^2 - S_{iy}^2) \{S_{jx}, S_{jy}\} - \\ &- \{S_{ix}, S_{iy}\} (S_{jx}^2 - S_{jy}^2)]. \end{aligned} \quad (31)$$

The Hamiltonian  $\hat{H}_{ch}$  describes two types of a longitudinal long-range diagonal  $Z$ -ordering measured by the static structure factors such as

$$\begin{aligned} S_{zz}(\mathbf{q}) &= \\ &= \frac{1}{N} \sum_{m,n} \exp\{-i\mathbf{q} \cdot (\mathbf{R}_m - \mathbf{R}_n)\} \langle S_{mz} S_{nz} \rangle \end{aligned} \quad (32)$$

for a pseudospin–dipole order and

$$S_{zz}^2(\mathbf{q}) = \frac{1}{N} \sum_{m,n} \exp\{-i\mathbf{q} \cdot (\mathbf{R}_m - \mathbf{R}_n)\} \langle S_{mz}^2 S_{nz}^2 \rangle \quad (33)$$

for a pseudospin–quadrupole (nematic) order.

The Hamiltonian  $\hat{H}_{tr}$  describes different types of transverse long-range off-diagonal XY-ordering measured by the transverse components of the static structure factors such as

$$S_{+-}(\mathbf{q}) = \frac{1}{N} \sum_{m,n} \exp\{-i\mathbf{q} \cdot (\mathbf{R}_m - \mathbf{R}_n)\} \langle S_{m+} S_{n-} \rangle \quad (34)$$

for the conventional pseudospin-dipole order or

$$T_{+-}(\mathbf{q}) = \frac{1}{N} \sum_{m,n} \exp\{-i\mathbf{q} \cdot (\mathbf{R}_m - \mathbf{R}_n)\} \langle T_{m+} T_{n-} \rangle, \quad (35)$$

and

$$S_{+-}^2(\mathbf{q}) = \frac{1}{N} \sum_{m,n} \exp\{-i\mathbf{q} \cdot (\mathbf{R}_m - \mathbf{R}_n)\} \langle S_{m+}^2 S_{n-}^2 \rangle \quad (36)$$

for two types of the pseudospin–quadrupole (nematic) order. In the conventional boson language, the structure factors  $S_{zz}(\mathbf{q})$  and  $S_{zz}^2(\mathbf{q})$  describe density–density correlations,  $S_{+-}(\mathbf{q})$  and  $T_{+-}(\mathbf{q})$  describe the single-boson superfluid correlations, while  $S_{+-}^2(\mathbf{q})$  describes the two-boson (on-site dimer) superfluid correlations.

#### 4. TYPICAL SIMPLIFIED $S = 1$ SPIN MODEL

Despite many simplifications, the effective pseudospin Hamiltonian (21) is rather complex, and represents one of the most general forms of the anisotropic  $S = 1$  non-Heisenberg Hamiltonian. Its real spin counterpart corresponds to an anisotropic  $S = 1$  magnet with a single-ion (on-site) and two-ion (inter-site bilinear and biquadratic) symmetric anisotropy in an external magnetic field under conservation of the total  $S_z$ . Spin Hamiltonian (21) describes an interplay of the Zeeman, single-ion, and two-ion anisotropic terms, giving rise to a competition of an (anti)ferromagnetic order along the  $Z$  axis with an in-plane  $XY$  magnetic order. Simplified versions of anisotropic  $S = 1$  Heisenberg Hamiltonian with bilinear exchange have been investigated rather extensively in recent years. Their analysis seems to provide an instructive introduction to the description of our generalized pseudospin model.

A typical  $S = 1$  spin Hamiltonian with uniaxial single-site and exchange anisotropies is given by

$$\hat{H} = \sum_{i>j} J_{ij}(S_{ix}S_{jx} + S_{iy}S_{jy} + \lambda S_{iz}S_{jz}) + \sum_i DS_{iz}^2 - \sum_i hS_{iz}. \quad (37)$$

The correspondence with our pseudospin Hamiltonian points to  $D = \Delta$ ,  $J_{ij} = t_{ij}$ , and  $\lambda J_{ij} = V_{ij}$ . The antiferromagnet with  $J > 0$  is usually considered because this is the case of more interest in general. However, Hamiltonian (37) is invariant under the transformation  $J, \lambda \rightarrow -J, -\lambda$  and a shift of the Brillouin zone  $\mathbf{k} \rightarrow \mathbf{k} + (\pi, \pi)$  for the square 2D lattice. The system described by Hamiltonian (2) can be characterized by local (on-site) spin-linear order parameters  $\langle \mathbf{S} \rangle$  and spin-quadratic (quadrupole spin-nematic) order parameters  $Q_0^2 = Q_{zz} = \langle S_z^2 - 2/3 \rangle$  and  $Q_{\pm 2}^2 = \langle S_{\pm 1}^2 \rangle$ .

The model has been studied by several methods, e. g., molecular field approximation, spin-wave theories, exact numerical diagonalizations, a nonlinear sigma model, quantum Monte Carlo, series expansions, variational methods, the coupled cluster approach, the self-consistent harmonic approximation, and the generalized SU(3) Schwinger boson representation [15–19].

The spectrum of spin Hamiltonian (37) in the absence of an external magnetic field changes drastically as  $\Delta$  varies from very small to very large positive or negative values. A strong “easy-plane” anisotropy for large positive  $\Delta > 0$  favors a singlet phase where spins are in the  $S_z = 0$  ground state. This “quadrupole” phase has no magnetic order, and is aptly referred to as a quantum paramagnetic phase (QPM), which is separated from the “ordered” state by a quantum critical point at some  $\Delta = \Delta_c^{QPM}$ . This is a quadrupole state with no magnetic order, and hence all linear order parameters vanish and only a quadrupole (spin-nematic) order parameter such as  $Q_{zz} = \langle S_z^2 - 2/3 \rangle$  is nonzero. The QPM phase consists of a unique ground state with the total spin  $S_z^{total} = 0$ , separated by a gap from the first excited states, which lie in the sectors  $S_z^{total} = \pm 1$ . It is worth noting that the QPM order differs in principle from the conventional paramagnetic state, because for  $S = 1$  in the classical paramagnetic state, we have  $\langle S_x^2 \rangle = \langle S_y^2 \rangle = \langle S_z^2 \rangle = 2/3$ , while in the quantum paramagnetic state,  $\langle S_z^2 \rangle = 0$  and  $\langle S_x^2 \rangle = \langle S_y^2 \rangle = 1$ . Strictly speaking, all the above analysis concerns the typical mean-field approximation (MFA). Beyond the MFA, the QPM ground state contains an admixture of states formed by exciton-like tightly bound particle–hole fluctuations (0 – 2 on nearby sites).

A strong “easy-axis” anisotropy for large negative

$\Delta \leq \Delta_c^{IS}$ ,  $\Delta_c^{IS} = 2(V_{nn}/t_{nn} - 1)$  [19], favors a spin ordering along  $z$ , the “easy axis”, with the on-site  $S_z = \pm 1$  ( $Z$ -phase). The order parameter is “Ising-like” and the long-range (staggered) diagonal order persists at finite temperatures, up to a critical line  $T_c(\Delta)$ . The easy axis antiferromagnetic  $Z_{AFM}$  phase or more complicated long-range spin  $Z$ -order are characterized by the longitudinal component of the static structure factor  $S_{zz}(\mathbf{q})$ .

For intermediate values  $\Delta_c^{QPM} > \Delta > \Delta_c^{IS}$ , the system is in a gapless XY phase, where the spins are preferentially in the  $xy$  plane (choosing  $z$  as the hard axis) and the Hamiltonian has the  $O(2)$  symmetry. At  $T = 0$ , this symmetry is spontaneously broken and the system exhibits spin order in some direction, reduced by quantum fluctuations. The broken  $O(2)$  symmetry results in a single gapless Goldstone mode. Although there is no ordered phase at a finite temperature, we expect a finite-temperature Kosterlitz–Thouless transition. The XY phase has a long-range off-diagonal ordering measured by the transverse component of the static structure factor  $S_{+-}(\mathbf{q})$ .

For large positive  $\Delta$ , in the QPM phase, the low-energy excitations arise from exciting one of the  $S_z = 0$  ( $n = 1$ ) sites to  $S_z = +1$  ( $n = 2$ ) or  $S_z = -1$  ( $n = 0$ ). Such a local excitation, actually the effective particle or hole, can then propagate over the lattice due to the transfer terms (quantum fluctuations) in  $H_{tr}$ , forming a well-defined quasiparticle (magnon) band with the energy  $\varepsilon(\mathbf{k})$ . These coherent magnon bands have an energy gap, which we expect to vanish as  $\Delta \rightarrow \Delta_c^{QPM}$ . An analytic expression for  $\varepsilon(\mathbf{k})$  in the QPM phase has been proposed by Papanicolaou [20], based on a generalized Holstein–Primakoff transformation for isotropic  $nn$ -Heisenberg model with single-site anisotropy. The application of an effective field  $h_z$  along the  $z$  axis reduces the spin gap linearly in  $h_z$  since the field couples to a conserved quantity (total spin along the  $z$  axis). The gap is closed at a critical field  $h_c$  (the quantum critical point (QCP)) where the bottom of the  $S_z = 1$  branch of (pseudo)spin excitations touches zero. This QCP belongs to the BEC universality class and the gapless mode of low-energy  $S_z = 1$  excitations remains quadratic for small momenta, because the Zeeman term commutes with the rest of the Hamiltonian.

Both excitation branches in the QPM phase,  $\Delta S_z = \pm 1$  (particle/hole), have the same dispersion at zero field,  $h_z = 0$ , as expected from time reversal symmetry. A finite  $h_z$  splits the branches linearly in  $h_z$ :  $\varepsilon_{\pm}(\mathbf{k}) \rightarrow \varepsilon_{\pm}(\mathbf{k}) \pm h_z$  without changing the dispersion. This is a consequence of the fact that the external field couples to the total spin  $\sum S_z$ , which is a conserved quantity.

We note that there are three types of two-magnon excitations, those with  $\Delta S_z^{total} = +2, -2$ , and  $0$ . The two-magnon bound state with  $\Delta S_z^{total} = 0$ , or a coupled particle–hole pair can propagate over the lattice, forming a quasiparticle band.

At least for relatively small negative  $\Delta < \Delta_c^{IS}$ , the lowest-energy excitations in the unperturbed system consist of a single spin excited from its ordered  $S_z = \pm 1$  state to  $S_z = 0$ , i. e.,  $\Delta S_z = \mp 1$ . The corresponding coherent magnon band has an energy gap at the  $\Gamma$  point  $(0, 0)$ , which behaves like  $\varepsilon(0, 0) \sim 2\sqrt{2V_{nn}|\Delta|}$  at small  $|\Delta|$ . This reflects, in the easy axis case, the fact that the residual  $O(2)$  symmetry of the Hamiltonian is not spontaneously broken in this case, and therefore Goldstone modes are absent.

However, for large negative  $\Delta$ , the single-magnon (single-particle) excitations are not the lowest-energy excitations of the system. Their energy is of the order of  $|\Delta|$ , whereas an excitation with  $\Delta S_z = \pm 2$  (i. e.,  $S_z = \pm 1 \leftrightarrow S_z = \mp 1$ ) has an energy of the order of  $2zV_{nn}$  as  $\Delta \rightarrow -\infty$ . Such a two-particle (local dimer) excitation, created at a particular site, can again propagate over the lattice, forming a quasiparticle band. We can think of this local dimer as a long-lived virtual two-magnon bound state (bimagnon), where the magnons are bound on the same site.

Hamer et al. [18] have shown that at a finite effective field  $h_z$  but at  $\lambda = 1$ , the XY phase transforms into a canted antiferromagnetic XY- $Z_{FM}$  phase that appears right above  $h_c$ : the spins acquire a uniform longitudinal component and an antiferromagnetically ordered transverse component, which spontaneously breaks the  $U(1)$  symmetry of global spin rotations along the  $z$  axis. The longitudinal magnetization increases with the field and saturates at the fully polarized (FP) state (all  $S_z = 1$ ) above the saturation field  $h_s$ . The FP state corresponds to a boson Mott insulator in the language of Bose gases.

The field-induced quantum phase transition from the QPM to the XY- $Z_{FM}$  phase is qualitatively different from the transition between the same two phases that is induced by changing  $\Delta$  at  $h_z = 0$ . If the single-ion anisotropy is continuously decreased at a zero applied field, the two excitation branches remain degenerate and the gap vanishes at  $\Delta = \Delta_c^{QPM}$  ( $h_z = 0$ ). The low-energy dispersion becomes linear at the QPM–CAFM phase boundary for small  $k$ . However, the degeneracy between the two branches at  $h_z = 0$  is lifted inside the CAFM phase: one of the branches remains gapless with a linear dispersion at low energy (corresponding to the Goldstone mode of the ordered CAFM state), whereas the other mode develops a gap to the lowest excitation. The effect of increasing  $h_z$  from zero

at a fixed  $\Delta > \Delta_c^{QPM}$  is to reduce the gap linearly in  $h_z$  with no change of dispersion.

At  $D > 0$  and  $\lambda > 1$ , the phase diagram of the  $S = 1$  Heisenberg model with uniaxial anisotropy (37) contains an extended spin supersolid (SS) or biconical phase XY- $Z_{FIM}$  with a ferrimagnetic  $z$ -order that does exist over a range of magnetic fields. The model also exhibits other interesting phenomena such as magnetization plateaus and a multicritical point [15]. The magnetization stays zero up to the critical field  $h_{c1}$  that marks a quantum phase transition (QPT) to a state with a finite fraction of spins in all the  $S_z = 0, \pm 1$  states. This spin supersolid state has a finite  $S_{zz}(\pi, \pi)$  as well as a finite  $S_{+-}(0, 0)$ . The magnetization increases continuously to  $m_z = 0.5$  at  $h_{c2}$ , where there is a second QPT to a second Ising-like state (IS2), where all the  $S_z = -1$  ( $n = 0$ ) sites have been flipped to the  $S_z = 0$  ( $n = 1$ ) state. The  $S_{zz}(\pi, \pi)$  component then remains divergent, but  $S_{+-}(0, 0)$  drops to zero. Upon further increasing the field, a first-order transition occurs to a pure XY-AFM phase (CAF) with the vanishing diagonal order but a finite  $S_{+-}(0, 0)$ . This situation persists until all the spins have flipped to the  $S_z = +1$  ( $n = 2$ ) state (fully polarized, FP phase). The extent of the SS phase decreases with decreasing  $\lambda$  and vanishes for  $\lambda \approx 1$ , leaving a second-order transition from the SS to the XY (CAF) phase.

At  $D < 0$ ,  $J > 0$ , and  $\lambda = 1$ , the ground state of spin Hamiltonian (37) corresponds to the easy-axis antiferromagnetic  $Z_{AFM}$  phase. At small anisotropy,  $|D|/J \leq 1$ , the application of an effective field  $h_z$  along the  $z$  axis first induces a rather conventional spin-flop transition to a pure XY-AFM phase (CAF) with the vanishing diagonal order but finite  $S_{+-}(0, 0)$ , ending with the transition to the fully polarized ferromagnetic  $Z_{FM}$  phase. However, at large anisotropy  $|D|/J \gg 1$ , instead of the mean-field first-order (metamagnetic) phase transition  $Z_{AFM}$ - $Z_{FM}$ , we arrive at an unconventional intermediate phase with the spin ferromagnetic (FNM) order characterized by zero value of the  $S_{+-}(0, 0)$  factor but a nonzero  $S_{+-}^2(0, 0)$  correlation function [16].

The phase diagram in the most interesting intermediate regime can change drastically, if we take frustrative effects of next-nearest-neighbor couplings or different non-Heisenberg biquadratic interactions into account [19]. We note that even for the simple isotropic 2D- $nnn$  antiferromagnetic Heisenberg model, the classical ground state has a Néel order only when  $J_2/J_1 < 1/2$ , where  $J_1$  is the nearest-neighbor and  $J_2$  is the next-nearest-neighbor interaction. However, when  $J_2/J_1 > 1/2$ , the ground state consists of two

independent sublattices with antiferromagnetic order. The classical ground-state energy does not depend on the relative orientations of both sublattices. However, quantum fluctuations lift this degeneracy and select a collinear order state, where the neighboring spins align ferromagnetically along one axis of the square lattice and antiferromagnetically along the other (stripe-like order).

Turning to spin-boson mapping, we note that the QPM phase ( $n_i = 1$ ), fully polarized  $Z_{FM}$  phases with  $n_i = 0$  or  $n_i = 2$  correspond to Mott insulating phases, the XY and XY- $Z_{FM}$  orderings correspond to a Bose-Einstein condensate (BEC) of single bosons, while the FNM phase corresponds the BEC of boson dimers. The XY- $Z_{FIM}$  phases correspond to supersolids.

The pseudospin Hamiltonian in Eqs. (21)–(24) differs from its simplified version (2) in several points. First, this concerns the density constraint. It is worth noting that the charge density constraint in a uniform pseudospin system can be satisfied only under some quasidegeneracy. Second, the pseudospin parameters, in particular  $\Delta$ ,  $V_{ij}$ , and  $h$  in effective Hamiltonian (21), can be closely linked to each other. Instead of a simple usually antiferromagnetic XY-exchange term in (2), we should proceed with a significantly more complicated form of the “transverse” term in the pseudospin Hamiltonian, (21), with the inclusion of two biquadratic terms and an unconventional “mixed” asymmetric ST-type term that formally breaks the time inversion symmetry and is absent for conventional spin Hamiltonians. The apparently leading bilinear XY-exchange term in  $\hat{H}_{tr}$  appears to be of the ferromagnetic sign. Along with a simple spin-linear planar XY-mode with nonzero  $\langle S_{\pm} \rangle$ , we arrive at two novel spin-quadrupole nematic modes with nonzero  $\langle T_{\pm} \rangle$  and/or  $\langle S_{\pm}^2 \rangle$ . Hereafter, we let the different counterparts of the phases of simple model (2) be denoted as follows: the novel XY-phase  $Z_{AFM}$  for Ising-type antiferromagnetic order along the  $z$  axis, XY- $Z_{FIM}$  for spin supersolid phases with simultaneous XY and ferrimagnetic orderings along the  $z$  axis, XY- $Z_{FM}$  for a phase with simultaneous XY- and ferromagnetic orderings along the  $z$  axis (an analogue of the CAFM phase), and  $Z_{FM}$  for the fully  $z$ -polarized ferromagnetic phase.

## 5. TOPOLOGICAL DEFECTS IN 2D $S = 1$ PSEUDOSPIN SYSTEMS

### 5.1. Short overview

In the framework of our model, the 2D Bose-Hubbard systems turn out to be in the universality class of the (pseudo)spin 2D systems whose descrip-

tion incorporates static or dynamic topological defects as a natural element of both micro- and macroscopic physics. Depending on the structure of the effective pseudospin Hamiltonian in 2D systems, these could correspond to either in-plane and out-of-plane vortices or skyrmions. Under certain conditions, either topological defects could determine the structure of the ground state. In particular, this could be a generic feature of electric multipolar systems with long-range multipolar interactions. Indeed, a Monte Carlo simulation of a ferromagnetic Heisenberg model with dipolar interaction on a 2D square  $L \times L$  lattice shows that as  $L$  is increased, the spin structure changes from a ferromagnetic one to a novel one with a vortex-like arrangement of spins even for rather small magnitude of dipolar anisotropy [21].

Topological defects are stable nonuniform spin structures with broken translational symmetry and a nonzero topological charge (chirality, vorticity, and winding number). Vortices are stable states of the anisotropic 2D Heisenberg Hamiltonian

$$\hat{H} = \sum_{i>j} J_{ij}(S_{ix}S_{jx} + S_{iy}S_{jy} + \lambda S_{iz}S_{jz}), \quad (38)$$

with the “easy-plane” anisotropy for the anisotropy parameter  $\lambda < 1$ . A classical in-plane vortex ( $S_z = 0$ ) appears to be a stable solution of classical Hamiltonian (38) at  $\lambda < \lambda_c$  ( $\lambda_c \approx 0.7$  for a square lattice). At  $1 > \lambda > \lambda_c$ , the stable solution corresponds to the out-of-plane OP vortex ( $S_z \neq 0$ ), at the center of which the spin vector appears to be oriented along the  $z$  axis, and at infinity it arranges within  $xy$  plane. The in-plane vortex is described by the formulas  $\Phi = q\varphi$ ,  $\cos \theta = 0$ . The  $\theta(r)$  dependence for the out-of-plane vortex cannot be found analytically. Both kinds of vortices have the energy logarithmically dependent on the size of the system.

The cylindrical domains, or bubble-like solitons with spins oriented along the  $z$  axis both at infinity and in the center (naturally, in opposite directions) exist for the “easy-axis” anisotropy  $\lambda > 1$ . Their energy has a finite value. Skyrmions are general static solutions of the classical continuous limit of the isotropic ( $\lambda = 1$ ) 2D Heisenberg ferromagnet, obtained by Belavin and Polyakov [22] from a classical nonlinear sigma model. The Belavin–Polyakov skyrmion and the out-of-plane vortex represent the simplest toy model of (pseudo)spin textures [22, 23].

The simplest skyrmion spin texture looks like a bubble domain in a ferromagnet and consists of a vortex-like arrangement of the in-plane components of spin with the  $z$ -component reversed in the centre of the

skyrmion and gradually increasing to match the homogeneous background at infinity. The spin distribution within such a classical skyrmion with a topological charge  $q$  is given by [22]

$$\Phi = q\varphi + \varphi_0, \quad \cos \Theta = \frac{r^{2q} - \lambda^{2q}}{r^{2q} + \lambda^{2q}}, \quad (39)$$

where  $r$  and  $\varphi$  are polar coordinates on the plane, and  $q = \pm 1, \pm 2, \dots$  is the chirality. For  $q = 1$  and  $\varphi_0 = 0$ , we arrive at

$$\begin{aligned} n_x &= \frac{2r\lambda}{r^2 + \lambda^2} \cos \varphi, & n_y &= \frac{2r\lambda}{r^2 + \lambda^2} \sin \varphi, \\ n_z &= \frac{r^2 - \lambda^2}{r^2 + \lambda^2}. \end{aligned} \quad (40)$$

In terms of the stereographic variables, the skyrmion with a radius  $\lambda$  and phase  $\varphi_0$  centered at a point  $z_0$  is identified with the spin distribution  $w(z) = \Lambda/(z - z_0)$ , where  $z = x + iy = re^{i\varphi}$  is a point in the complex plane,  $\Lambda = \lambda e^{i\alpha}$ . For a multicenter skyrmion, we have [22]

$$\begin{aligned} w(z) &= \text{ctg} \frac{\Theta}{2} e^{i\Phi} = \\ &= \prod_i \left( \frac{z - z_i}{\Lambda} \right)^{m_i} \prod_j \left( \frac{\Lambda}{z - z_j} \right)^{n_j}, \end{aligned} \quad (41)$$

where  $\sum m_i > \sum n_j$ ,  $q = \sum m_j$ . Skyrmions are characterized by the magnitude and the sign of their topological charge, by their size (radius), and by the global orientation of the spin. The scale invariance of a skyrmionic solution reflects in that its energy  $E_{sk} = 4\pi|q|IS^2$  is proportional to the topological charge and does not depend on the radius and the global phase [22]. Like domain walls, vortices and skyrmions are stable for topological reasons. Skyrmions cannot decay into other configurations because of this topological stability, irrespective of how close they are in energy to any other configuration.

In a continuous field model, such as, e.g., the nonlinear  $\sigma$ -model, the ground-state energy of the skyrmion is independent of its size [22], but for the skyrmion on a lattice, the energy depends on its size. This must lead to a collapse of the skyrmion, making it unstable. Strong anisotropic interactions, in particular, long-range dipole–dipole interactions may in principle dynamically stabilize the skyrmions in 2D lattices [24].

The wave function of the spin system that corresponds to a classical skyrmion is a product of spin coherent states [25]. For the spin  $S = 1/2$ ,

$$\begin{aligned} \Psi_{sk}(0) &= \\ &= \prod_i \left[ \cos \frac{\theta_i}{2} e^{i\varphi_i/2} | \uparrow \rangle + \sin \frac{\theta_i}{2} e^{-i\varphi_i/2} | \downarrow \rangle \right], \end{aligned} \quad (42)$$

where  $\theta_i = \arccos \frac{r_i^2 - \lambda^2}{r_i^2 + \lambda^2}$ . The coherent state provides a maximal equivalence to a classical state with the minimal uncertainty of spin components. The motion of such skyrmions has to be of a highly quantum mechanical nature. However, this may involve a semiclassical percolation in the case of heavy nonlocalized skyrmions or variable range hopping in the case of highly localized skyrmions in a random potential. Effective overlap and transfer integrals for quantum skyrmions are calculated analytically in [26]. The skyrmion motion has a cyclotron character and resembles that of the electron in a magnetic field.

The interest in skyrmions in ordered spin systems received much attention soon after the discovery of high-temperature superconductivity in copper oxides [27, 28]. Initially, there was some hope that interaction of electrons and holes with spin skyrmions could play some role in superconductivity, but this was never successfully demonstrated. Some indirect evidence of skyrmions in the magnetoresistance of the lithium-doped lanthanum copper oxide has been recently reported [29], but direct observation of skyrmions in 2D antiferromagnetic lattices is still lacking. In recent years, the skyrmions and exotic skyrmion crystal (SkX) phases have been discussed in relation with a wide range of condensed matter systems including the quantum Hall effect, spinor Bose condensates, and especially chiral magnets [30]. It is worth noting that the skyrmion-like structures for hard-core 2D boson system were considered by Moskvin *et al.* [31] in the framework of the  $S = 1/2$  pseudospin formalism.

### 5.2. Unconventional skyrmions in $S = 1$ (pseudo)spin systems

Different skyrmion-like topological defects for 2D (pseudo)spin  $S = 1$  systems as solutions of isotropic spin Hamiltonians were addressed in Ref. [12] and in more detail in Ref. [11]. In general, an isotropic non-Heisenberg spin Hamiltonian for the  $S = 1$  quantum (pseudo)spin systems should include both the bilinear Heisenberg exchange term and the biquadratic non-Heisenberg exchange term:

$$\begin{aligned} \hat{H} &= -\tilde{J}_1 \sum_{i,\eta} \hat{S}_i \hat{S}_{i+\eta} - \tilde{J}_2 \sum_{i,\eta} (\hat{S}_i \hat{S}_{i+\eta})^2 = \\ &= -J_1 \sum_{i,\eta} \hat{S}_i \hat{S}_{i+\eta} - \\ &- J_2 \sum_{i,\eta} \sum_{k \geq j}^3 (\{\hat{S}_k \hat{S}_j\}_i \{\hat{S}_k \hat{S}_j\}_{i+\eta}), \end{aligned} \quad (43)$$

where  $J_i$  are the appropriate exchange integrals,  $J_1 = \tilde{J}_1 - \tilde{J}_2/2$ ,  $J_2 = \tilde{J}_2/2$ , and  $i$  and  $\eta$  denote respective summations over lattice sites and nearest neighbors.

With our trial wave function (8) substituted in  $\langle \hat{H} \rangle$  under the condition  $\langle \hat{S}(1) \hat{S}(2) \rangle = \langle \hat{S}(1) \rangle \langle \hat{S}(2) \rangle$ , we arrive at the Hamiltonian of the isotropic classical spin-1 model in the continual approximation in the form

$$\begin{aligned} H &= J_1 \int d^2 \mathbf{r} \left[ \sum_{i=1}^3 (\nabla \langle \hat{S}_i \rangle)^2 \right] + \\ &+ J_2 \int d^2 \mathbf{r} \left[ \sum_{i \geq j=1}^3 (\nabla a_i a_j + \nabla b_i b_j)^2 \right] + \\ &+ \frac{4(J_2 - J_1)}{c^2} \int |\langle \hat{S} \rangle|^2 d^2 \mathbf{r}, \end{aligned} \quad (44)$$

where  $\langle \hat{S} \rangle = 2[\mathbf{a} \times \mathbf{b}]$ . We note that the third “gradient-free” term in the Hamiltonian breaks the scaling invariance of the model.

#### 5.2.1. Dipole (pseudo)spin skyrmions

Dipole, or magnetic skyrmions as solutions of the bilinear Heisenberg (pseudo)spin Hamiltonian with  $J_2 = 0$  were obtained in Ref. [12] under the restriction  $\mathbf{a} \perp \mathbf{b}$  and for fixed lengths of these vectors.

The model reduces to the nonlinear  $O(3)$ -model with the solutions for  $\mathbf{a}$  and  $\mathbf{b}$  described (in polar coordinates) as

$$\begin{aligned} \sqrt{2} \mathbf{a} &= (\mathbf{e}_z \sin \theta - \mathbf{e}_r \cos \theta) \sin \varphi + \mathbf{e}_\varphi \cos \varphi, \\ \sqrt{2} \mathbf{b} &= (\mathbf{e}_z \sin \theta - \mathbf{e}_r \cos \theta) \cos \varphi - \mathbf{e}_\varphi \sin \varphi. \end{aligned} \quad (45)$$

For dipole “magneto-electric” skyrmions, the  $\mathbf{m}$  and  $\mathbf{n}$  vectors are assumed to be perpendicular to each other ( $\mathbf{m} \perp \mathbf{n}$ ) and the (pseudo)spin structure is determined by skyrmion distribution (39) of the  $\mathbf{l} = [\mathbf{m} \times \mathbf{n}]$  vector [12]. In other words, the fixed-length spin vector  $\langle \hat{S} \rangle = 2[\mathbf{a} \times \mathbf{b}]$  is distributed in the same way as for the usual skyrmions in (39). But unlike the usual classic skyrmions, the dipole skyrmions in the  $S = 1$  theory have an additional topological structure due to the existence of two vectors  $\mathbf{m}$  and  $\mathbf{n}$ . In going around the center of the skyrmion, the vectors can make  $N$  turns around the  $\mathbf{l}$  vector. Thus, we can introduce two topological quantum numbers,  $N$  and  $q$  [12]. In addition, we note that the  $q$  number may be half-integer. The dipole–quadrupole skyrmion is characterized by a nonzero both pseudospin dipole order parameter  $\langle \hat{S} \rangle$  with the usual skyrmion texture (39) and quadrupole order parameters

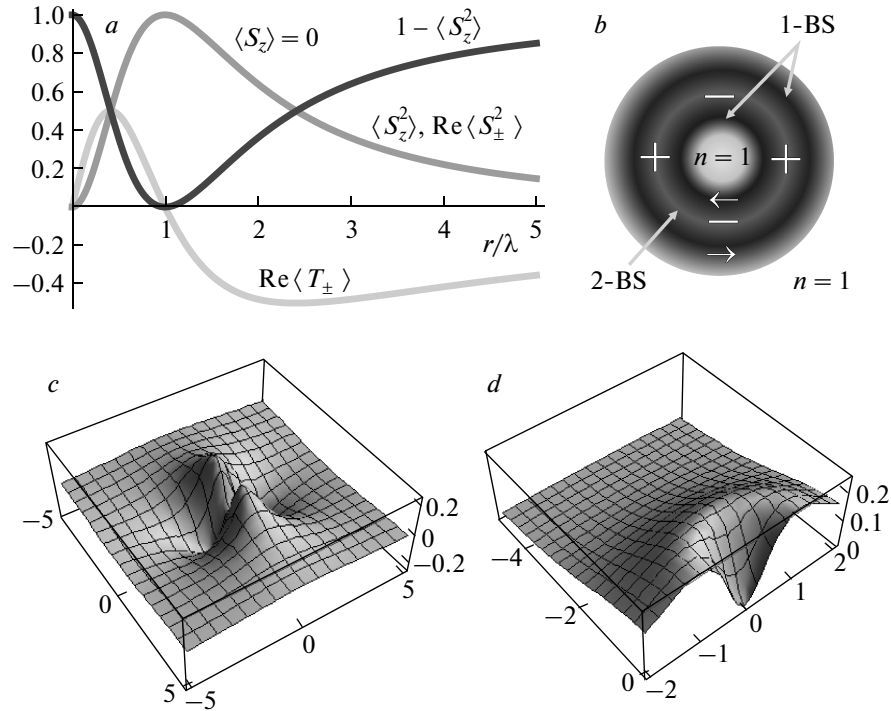


**Fig. 2.** *a)* Radial distribution of the boson nematic order parameters for a quadrupole pseudospin skyrmion ( $q = 1$ ) with  $\langle n_i \rangle = n = 1$  ( $\varphi = 0$ ): *b)* the ring-shaped distribution of the one- and two-boson SF order parameters: *c)* and *d)* the spatial distribution of  $\text{Re} \langle \hat{S}_{\pm}^2 \rangle$  and  $\langle \hat{S}_z^2 \rangle$ , respectively

$$\langle \{\hat{S}_i \hat{S}_j\} \rangle = 2 \langle \hat{S}_i \rangle \langle \hat{S}_j \rangle = l_i l_j. \quad (46)$$

### 5.2.2. Quadrupole (pseudo)spin skyrmions

Hereafter, we address another situation with a purely biquadratic (pseudo)spin Hamiltonian ( $J_1 = 0$ ) and treat the nonmagnetic (“electric”) degrees of freedom. The topological classification of purely electric solutions is simple because it is based on the use of a subgroup instead of the full group. We address the solutions with  $\mathbf{a} \parallel \mathbf{b}$  and with fixed lengths of the vectors, and therefore we can use the same subgroup as above for classification.

After simple algebra, the biquadratic part of the Hamiltonian can be reduced to the expression familiar from the nonlinear  $O(3)$ -model:

$$\begin{aligned} H_{bq} &= J_2 \int d^2 \mathbf{r} \left[ \sum_{i,j=1}^3 (\nabla n_i n_j)^2 \right] = \\ &= 2J_2 |\mathbf{n}|^2 \int d^2 \mathbf{r} \left[ \sum_{i=1}^3 (\nabla n_i)^2 \right], \quad (47) \end{aligned}$$

where  $\mathbf{a} = \alpha \mathbf{n}$ ,  $\mathbf{b} = \beta \mathbf{n}$ , and  $\alpha + i\beta = \exp(i\kappa)$ ,  $\kappa \in R$ ,  $|\mathbf{n}|^2 = \text{const}$ . Its solutions are skyrmions, but instead

of the spin distribution in magnetic skyrmion, we here have solutions with zero spin but a nonzero distribution of five spin-quadrupole moments  $Q_{ij}$ , or  $\langle \{S_i S_j\} \rangle$ , which are in turn determined by the “skyrmionic” distribution of the  $\mathbf{n}$  vector in (39) with the classical skyrmion energy  $E_{el} = 16\pi q J_2$ . The distribution of the spin-quadrupole moments  $\langle \{S_i S_j\} \rangle$  can be easily obtained as

$$\begin{aligned} \langle S_z^2 \rangle &= \frac{4r^{2q} \lambda^{2q}}{(r^{2q} + \lambda^{2q})^2}, \\ \langle \hat{S}_{\pm}^2 \rangle &= \frac{2r^{2q} \lambda^{2q}}{(r^{2q} + \lambda^{2q})^2} e^{\pm 2iq\varphi}, \quad (48) \\ \langle \hat{T}_{\pm} \rangle &= -i\sqrt{2} \frac{(\lambda^{2q} - r^{2q}) r^q \lambda^q}{(r^{2q} + \lambda^{2q})^2} e^{\mp iq\varphi}. \end{aligned}$$

We emphasize that the distribution of five independent quadrupole order parameters for the quadrupole skyrmion are straightforwardly determined by a single vector field  $\mathbf{m}(\mathbf{r})$  ( $\mathbf{n}(\mathbf{r})$ ) while  $\langle \hat{\mathbf{S}} \rangle = 0$ .

Figure 2 demonstrates the radial distribution of different (pseudo)spin order parameters for the quadrupole skyrmion. We see a circular layered structure with clearly visible anticorrelation effects due to the (pseudo)spin kinematics. Interestingly, at

the center ( $r = 0$ ) and far from the center ( $r \rightarrow \infty$ ) for such a skyrmion, we deal with an  $M = 0$ , or Mott insulating state, while in the domain wall center ( $r = \lambda$ ), we arrive at an  $M = \pm 1$  superposition with the maximal value of the  $|\langle \hat{S}_{\pm}^2 \rangle|$  parameter, whose weight diminishes in moving away from the center. The  $|\langle \hat{T}_{\pm} \rangle|$  parameter vanishes at the domain wall center  $r = \lambda$ , at the skyrmion center  $r = 0$ , and at the infinity  $r \rightarrow \infty$  ( $\propto \frac{1}{r}$ ), with the two extremums at  $r = \frac{\lambda}{\sqrt{2 \pm 1}}$ . In other words, we arrive at a very complicated interplay of single- and two-boson superfluids with density maxima at  $r = \frac{\lambda}{\sqrt{2 \pm 1}}$  and at the domain wall center ( $r = \lambda$ ). The ring-shaped domain wall is an area with a circular distribution of the superfluid order parameters, or a circular “bosonic” supercurrent. A nonzero  $T$ -type order parameter distribution points to a circular “one-boson” current with a puzzlingly opposite sign ( $\pi$  phase difference) of the  $\langle \hat{T}_{\pm} \rangle$  parameter for the “internal” ( $0 < r < \lambda$ ) and “external” ( $r > \lambda$ ) parts of the skyrmion, while the  $\langle \hat{S}_{\pm}^2 \rangle$  parameter defines the two-boson, or dimer superfluid order. The specific spatial separation of different order parameters that avoid each other reflects the competition of different  $k, j$  terms in (43). Given the simplest winding number  $q = 1$ , we arrive at the  $p$  or  $d$ -wave ( $d_{x^2-y^2}/d_{xy}$  in-plane symmetry of the one-boson or dimer superfluid order parameters).

One of the most exciting features of the quadrupole skyrmion is that such a skyrmionic structure is characterized by a uniform distribution of the mean on-site boson density  $\langle n_i \rangle = n = 1$  for  $\langle \hat{S}_{iz} \rangle = 0$ . In other words, the quadrupole skyrmionic structure and the bare “parent” Mott insulating phase have absolutely the same distribution of the mean on-site densities. On one hand, this point underlines an unconventional quantum nature of the quadrupole skyrmion under consideration, while on the other hand, it makes the quadrupole skyrmion texture an “invisible being” for several experimental techniques. However, the domain-wall center of the quadrupole skyrmion appears to reveal maximal values of the pseudospin susceptibility  $\chi_{zz}$  [31]. This means that the domain wall appears to form a very efficient ring-shaped potential well for the boson localization, thus giving rise to a novel type of a “charged” topological defect. In the framework of the pseudospin formalism, the “charging” of a bare “neutral” skyrmion corresponds to a single-magnon  $\Delta S_z = \pm 1$  (single particle) or a two-magnon  $\Delta S_z = \pm 2$  (two-particle) dimer excitations. It is worth noting that for large negative  $\Delta$ , the single-magnon (single-particle) excitations may not be the lowest-energy excitations of the strongly anisotropic pseudospin system. Their energy

may surpass the energy of a two-magnon bound state (bimagnon), or the two-boson dimer excitation created at a particular site. Thus we arrive at a competition of two types of “charged” quadrupole skyrmions with  $\Delta N = \pm 1$  and  $\Delta N = \pm 2$  ( $\Delta N$  is the total number of bosons). Such a “charged” topological defect can be addressed as an extended skyrmion-like mobile quasiparticle. However, it must be borne in mind that skyrmion corresponds to a collective state (excitation) of the whole system.

Addition or removal of a boson in the half-filled ( $n = 1$ ) boson system can be a driving force for the nucleation of multi-center “charged” skyrmions. Such *topological* structures, rather than uniform phases predicted by the mean-field approximation, are believed to describe the evolution of the EBHM systems away from half-filling. It is worth noting that the multi-center skyrmions are considered as systems of skyrmion-like quasiparticles forming skyrmion liquids and skyrmion lattices, or crystals (see, e. g., Refs. [32, 33]).

### 5.2.3. Dipole-quadrupole (pseudo)spin skyrmions

In the continual limit with  $J_1 = J_2 = J$ , Hamiltonian (44) can be transformed into the classical Hamiltonian of the fully  $SU(3)$ -symmetric scale-invariant model, which can be rewritten as [11]

$$H_{isotr} = 2J \int d^2 \mathbf{r} \{ (\nabla \Theta)^2 + \sin^2 \Theta (\nabla \eta)^2 + \sin^2 \Theta \cos^2 \Theta [\cos^2 \eta (\nabla \Psi_1)^2 + \sin^2 \eta (\nabla \Psi_2)^2] + \sin^4 \Theta \cos^2 \eta \sin^2 \eta (\nabla \Psi_1 - \nabla \Psi_2)^2 \}, \quad (49)$$

where we use representation (6) and set  $\Psi_1 = \Phi_1 - \Phi_3$ ,  $\Psi_2 = \Phi_3 - \Phi_2$ . The topological solutions for Hamiltonian (49) can be classified by three topological quantum numbers (winding numbers) at least: the phases  $\eta$  and  $\Psi_{1,2}$  can change by  $2\pi$  after passing around the center of the defect. The appropriate modes may have a very complicated topological structure due to the possibility for one defect to have several different centers (while one of the phases  $\eta$ ,  $\Psi_{1,2,3}$  changes by  $2\pi$  under one turn around one center  $(r_1, \varphi_1)$ , other phases may pass around other centers  $(r_i, \varphi_i)$ ). We note that for such a center, the winding numbers may take half-integer values. Hence, we arrive at a large variety of topological structures representing solutions of the model. Below, we briefly address two simplest classes of such solutions. One type of skyrmions can be obtained for the trivial phases  $\Psi_{1,2}$ . If these are constant, the  $\mathbf{R}$  vector distribution (see (6)) represents a skyrmion described by the usual formula (39). All but one topo-

logical quantum numbers are zero for this class of solutions. It includes both dipole and quadrupole solutions: depending on the selected constant phases, we can obtain both “electric” and different “magnetic” skyrmions. The substitution  $\Phi_1 = \Phi_2 = \Phi_3$  leads to the electric skyrmion that was obtained above as a solution of a more general SU(3)-anisotropic model. Another example is given by  $\Phi_1 = \Phi_2 = 0$ ,  $\Phi_3 = \pi/2$ . This substitution implies that  $\mathbf{b} \parallel z$ ,  $\mathbf{a} \parallel xy$ ,  $\mathbf{S} \parallel xy$ , and  $\mathbf{S} = \sin \Theta \cos \Theta \{\sin \eta, -\cos \eta, 0\}$ . Nominally, this is an in-plane spin vortex with a varying length of the spin vector

$$|S| = \frac{2r\lambda|r^2 - \lambda^2|}{(r^2 + \lambda^2)^2},$$

which is zero at the circle  $r = \lambda$ , at the center  $r = 0$ , and at the infinity  $r \rightarrow \infty$ , and has maxima at  $r = \lambda(\sqrt{2} \pm 1)$ . In addition to the nonzero in-plane components of the spin-dipole moment  $\langle S_{x,y} \rangle$ , this vortex is characterized by a nonzero distribution of (pseudo)spin-quadrupole moments. We emphasize the difference between spin-1/2 systems, in which there are solutions such as in-plane vortices with the energy having a well-known logarithmic dependence on the size of the system and a fixed spin length, and spin-1 systems, in which the in-plane vortices can also exist but can have a finite energy and a varying spin length. The distribution of quadrupole components associated with an in-plane spin-1 vortex is nontrivial. Such solutions can be termed “in-plane dipole-quadrupole skyrmions”.

Other types of the simplest solutions with the phases  $\Psi_1 = Q_1\varphi$ ,  $\Psi_2 = Q_2\varphi$  governed by two integer winding numbers  $Q_{1,2}$  and  $\eta = \eta(r)$ ,  $\Theta = \Theta(r)$  are considered in Ref. [11].

## 6. CONCLUSION

The pseudospin formalism is shown to constitute a powerful method for studying complex phenomena in interacting quantum systems. We have focused here on the most prominent and intensively studied  $S = 1$  pseudospin formalism for the extended boson Hubbard model with truncation of the on-site Hilbert space to the three lowest occupation states  $n = 0, 1, 2$ . The EHBH Hamiltonian is a paradigmatic model for the highly topical field of ultracold gases in optical lattices. At variance with the standard EHBH Hamiltonian, which seems to be insufficient for quantitatively describing the physics of boson systems, the generalized non-Heisenberg effective pseudospin Hamiltonian in Eqs. (21)–(24) provides a deeper link with boson system and a physically clear description of

“the myriad of phases”, from uniform Mott insulating phases and density waves to two types of superfluids and supersolids. The Hamiltonian could provide a novel starting point for analytic and computational studies of semi-hard core boson systems. Furthermore, we argue that the 2D  $S = 1$  pseudospin system is prone to a topological phase separation and address different types of unconventional skyrmion-like structures, which, to the best of our knowledge, have not been analyzed until now. The structures are characterized by a complicated interplay of the insulating and two superfluid phases with a single boson and boson dimers condensation. We also discussed the skyrmions as classical solutions of the continual isotropic models; however, this idealized object is believed to preserve its main features for strongly anisotropic (pseudo)spin lattice quantum systems. Strictly speaking, the continuous model is relevant for discrete lattices only if we deal with long-wavelength inhomogeneities whose size is much larger than the lattice spacing. In a discrete lattice, the very notion of a topological excitation seems to be inconsistent. At the same time, both quantum effects and the discreteness of the lattice itself do not prohibit considering the nanoscale (pseudo)spin textures whose topology and spin arrangement are those of a skyrmion [27, 28].

We thank A. B. Borisov and Yu. D. Panov for the useful discussions. The research was supported by the Government of the Russian Federation, Program 02.A03.21.0006 and by the Ministry of Education and Science of the Russian Federation, projects Nos. 1437 and 2725.

## REFERENCES

1. M. P. A. Fisher et al., Phys. Rev. B **40**, 546 (1989); Subir Sachdev, *Quantum Phase Transitions*, Cambridge Univ. Press, Cambridge (2001); O. Dutta, M. Gajda, P. Hauke, M. Lewenstein, D.-S. Lühmann, B. A. Malomed, T. Sowiński, and J. Zakrzewski, arXiv:1406.0181.
2. Kwai-Kong Ng and Min-Fong Yang, Phys. Rev. B **83**, 100511(R) (2011).
3. Ehud Altman and Assa Auerbach, Phys. Rev. Lett. **89**, 250404 (2002); Erez Berg, Emanuele G. Dalla Torre, Thierry Giamarchi, and Ehud Altman, Phys. Rev. B **77**, 245119 (2008); L. Mazza, M. Rizzi, M. Lewenstein, and J. I. Cirac, Phys. Rev. A **82**, 043629 (2010).
4. T. Matsubara and H. Matsuda, Prog. Theor. Phys. **16**, 569 (1956).

5. C. D. Batista and G. Ortiz, *Adv. Phys.* **53**, 1 (2004).
6. P. Jordan and E. Wigner, *Z. Physik*, **47**, 631 (1928).
7. T. Holstein and H. Primakoff, *Phys. Rev.* **58**, 1098 (1940).
8. A. S. Moskvina, *Phys. Rev. B* **84**, 075116 (2011).
9. A. S. Moskvina, *J. Phys.: Condens. Matter* **25**, 085601 (2013).
10. D. A. Varshalovich, A. N. Moskalev, and V. K. Khersonskii, *Quantum Theory of Angular Momentum*, World Scientific, Singapore, (1988).
11. N. A. Mikushina and A. S. Moskvina, *Phys. Lett. A* **302**, 8 (2002); arXiv:cond-mat/0111201.
12. A. Knigavko, B. Rosenstein, and Y. F. Chen, *Phys. Rev. B* **60**, 550 (1999).
13. M. Blume, *Phys. Rev.* **141**, 517 (1966); H. W. Capel, *Physica (Utrecht)* **32**, 966 (1966).
14. J. E. Hirsch and S. Tang, *Phys. Rev. B* **40**, 2179 (1989); J. E. Hirsch, in: *Polarons and Bipolarons in High- $T_c$  Superconductors and Related Materials*, ed. by E. K. H. Salje, A. S. Alexandrov, and W. Y. Liang, Cambridge Univ. Press, Cambridge (1995), p. 234.
15. P. Sengupta and C. D. Batista, *Phys. Rev. Lett.* **98**, 227201 (2007); *J. Appl. Phys.* **103**, 07C709 (2008).
16. K. Wierschem, Y. Kato, Y. Nishida, C. D. Batista, and P. Sengupta, *Phys. Rev. B* **86**, 201108(R) (2012).
17. M. R. H. Khajepour, Yung-Li Wang, and R. A. Kromhout, *Phys. Rev. B* **12**, 1849 (1975).
18. J. Oitmaa and C. J. Hamer, *Phys. Rev. B* **77**, 224435 (2008); C. J. Hamer, O. Rojas, and J. Oitmaa, *Phys. Rev. B* **81**, 214424 (2010).
19. R. S. Lapa and A. S. T. Pires, *J. Magn. Magn. Mater.* **327**, 1 (2013); A. S. T. Pires, *Sol. St. Comm.* **152**, 1838 (2012).
20. N. Papanicolau, *Phys. Lett. A* **116**, 89 (1986); *Nucl. Phys.* **305**, 367 (1988).
21. J. Sasaki and F. Matsubara, *J. Phys. Soc. Jpn.* **66**, 2138 (1997).
22. A. A. Belavin and A. M. Polyakov, *JETP Lett.* **22**, 245 (1975).
23. A. B. Borisov, S. A. Zykov, N. A. Mikushina, and A. S. Moskvina, *Phys. Sol. St.* **44**, 324 (2002).
24. Ar. Abanov and V. L. Pokrovsky, *Phys. Rev. B* **58**, R8889 (1998); B. A. Ivanov, A. Y. Merkulov, V. A. Stephanovich, and C. E. Zaspel, *Phys. Rev. B* **74**, 224422 (2006); E. G. Galkina, E. V. Kirichenko, B. A. Ivanov, and V. A. Stephanovich, *Phys. Rev. B* **79**, 134439 (2009).
25. A. M. Perelomov, *Generalized Coherent States and Their Applications*, Springer-Verlag, Berlin (1986).
26. R. A. Istomin and A. S. Moskvina, *JETP Lett.* **71**, 338 (2000).
27. P. B. Wiegmann, *Phys. Rev. Lett.* **60**, 821 (1988); B. I. Shraiman and E. D. Siggia, *Phys. Rev. Lett.* **61**, 467 (1988); X. G. Wen and A. Zee, *Phys. Rev. Lett.* **61**, 1025 (1988); S. Chakravarty, B. I. Halperin, and D. R. Nelson, *Phys. Rev. B* **39**, 2344 (1989); P. Voruganti and S. Doniach, *Phys. Rev. B* **41**, 9358 (1990); R. J. Gooding, *Phys. Rev. Lett.* **66**, 2266 (1991); S. Haas, F.-C. Zhang, F. Mila, and T. M. Rice, *Phys. Rev. Lett.* **77**, 3021 (1996).
28. E. C. Marino and M. B. Silva Neto, *Phys. Rev. B* **64**, 092511 (2001); T. Morinari, *Phys. Rev. B* **65**, 064513 (2002); T. Morinari, *Phys. Rev. B* **72**, 104502 (2005); Z. Nazario and D. I. Santiago, *Phys. Rev. Lett.* **97**, 197201 (2006).
29. I. Raicevic, D. Popovic, C. Panagopoulos, L. Benfatto, M. B. Silva Neto, E. S. Choi, and T. Sasagawa, *Phys. Rev. Lett.* **106**, 227206 (2011).
30. A. Bogdanov and A. Hubert, *J. Magn. Magn. Mater.* **138**, 255 (1994); U. K. Rossler, A. Bogdanov, and C. Pfleiderer, *Nature* **442**, 797801 (2006); N. Nagaosa and Y. Tokura, *Nature Nanotechnology* **8**, 899 (2013).
31. A. S. Moskvina, I. G. Bostrem, and A. S. Ovchinnikov, *JETP Lett.* **78**, 772 (2003); A. S. Moskvina, *Phys. Rev. B* **69**, 214505 (2004).
32. C. Timm, S. M. Girvin, and H. A. Fertig, *Phys. Rev. B* **58**, 10634 (1998).
33. A. G. Green, *Phys. Rev. B* **61**, R16299 (2000).